Cysteine as an Innovative Biomarker for Kidney Injury

Hye Young Woo, MD,[1] Jong Min An, PhD,[2] Min Young Park, BS,[1] Ahram Han, MD,[1] Youngwoong Kim, MS,[2] Jisoo Kang, MS,[2] Sanghyun Ahn, MD, PhD,[1] Seung-Kee Min, MD, PhD,[1] Jongwon Ha, MD, PhD, [1] Dokyoung Kim, PhD,[2,3,4,5,6,7,8,9] and Sangil Min, MD, PhD[1]

Background. Kidney transplantation is a widely used treatment for end-stage kidney disease. Nevertheless, the incidence of acute kidney injury (AKI) in deceased donors poses a potential hazard because it significantly increases the risk of delayed graft function and potentially exerts an influence on the kidney allograft outcome. It is crucial to develop a diagnostic model capable of assessing the existence and severity of AKI in renal grafts. However, no suitable kidney injury markers have been developed thus far. **Methods.** We evaluated the efficacy of the molecular probe NPO-B, which selectively responds to cysteine, as a new diagnostic tool for kidney injury. We used an in vitro model using ischemia/reperfusion injury human kidney-2 cells and an in vivo ischemia/reperfusion injury mouse model. Additionally, cysteine was investigated using urine samples from deceased donors and living donors to assess the applicability of detection techniques to humans. **Results.** This study confirmed that the NPO-B probe effectively identified and visualized the severity of kidney injury by detecting cysteine in both in vitro and in vivo models. We observed that the fluorescence intensity of urine samples measured using NPO-B from the deceased donors who are at a high risk of renal injury was significantly stronger than that of the living donors. **Conclusions.** If implemented in clinical practice, this new diagnostic tool using NPO-B can potentially enhance the success rate of kidney transplantation by accurately determining the extent of AKI in renal grafts.

(*Transplantation* 2024;00: 00–00).

Received 9 October 2023. Revision received 18 May 2024.

Accepted 21 May 2024.

[1] Department of Surgery, Seoul National University College of Medicine, Seoul, Republic of Korea.

[2] Department of Biomedical Science, Graduate School, Kyung Hee University, Seoul, Republic of Korea.

[3] Medical Research Center for Bioreaction to Reactive Oxygen Species and Biomedical Science Institute, Core Research Institute (CRI), Kyung Hee University, Seoul, Republic of Korea.

[4] Department of Anatomy and Neurobiology, College of Medicine, Kyung Hee University, Seoul, Republic of Korea.

[5] Center for Converging Humanities, Kyung Hee University, Seoul, Republic of Korea.

[6] KHU-KIST Department of Converging Science and Technology, Kyung Hee University, Seoul, Republic of Korea.

[7] UC San Diego Materials Research Science and Engineering Center, La Jolla, CA.

[8] Center for Brain Technology, Brain Science Institute, Korea Institute of Science and Technology, Seoul, Republic of Korea.

[9] Department of Precision Medicine, Graduate School, Kyung Hee University, Seoul, Republic of Korea.

This research was supported by a grant from the Korea Health Technology R&D Project of the Korea Health Industry Development Institute funded by the Bio and Medical Technology Development Program of the National Research Foundation (NRF) of Korea funded by the Ministry of Science and Information and Communication Technology (grant 2021-M3A9I5030523; D.K.). This research was also supported by the Basic Science Research Program through the NRF of Korea funded by the Ministry of Education (grant 2018-R1A6A1A03025124; D.K.), and an NRF grant funded by the Korean government (Ministry of Science and Information and Communication Technology; grant 2022-R1F1A1069954; D.K. and grant 2021-R1F1A1059888; S.M.).

The authors are listed as inventors on a pending patent application related to the technology described in this work.

H.Y.W., D.K., S.M., and J.M.A. conceived the work. Y.K. synthesized NPO-B and performed the in vitro and urine analyses. H.Y.W. performed prediction analysis. A.H., S.A., S-K.M., and J.H. evaluated and discussed the data. H.Y.W., J.M.A., M.Y.P., J.K., and S.M. performed in vivo and ex vivo analyses. H.Y.W., J.M.A., D.K., and S.M. wrote the article. D.K. and S.M. provided advice and oversaw the execution of this work.

H.Y.W. and J.M.A. share first authorship.

The authors declare that the data supporting the findings of this study are available within the article and its supplementary information or from the corresponding authors (S.M. and D.K.) on reasonable request.

The funder had no role in the study design, data collection and analysis, decision to publish, or article preparation.

Supplemental visual abstract; http://links.lww.com/TP/D116.

Supplemental digital content (SDC) is available for this article. Direct URL citations appear in the printed text, and links to the digital files are provided in the HTML text of this article on the journal's Web site (www.transplantjournal.com).

Correspondence: Sangil Min, M.D., PhD, Division of Transplantation and Vascular Surgery, Department of Surgery, Seoul National University Hospital, 101, Daehak-ro, Jongno-gu, Seoul 03080, Republic of Korea. (surgeonmsi@gmail.com); Dokyoung Kim, PhD, Department of Biomedical Science, Graduate School, Kyung Hee University, 26 Kyungheedae-Ro, Dongdaemun-Gu, Seoul 02447, Republic of Korea. (dkim@khu.ac.kr).

ISSN: 0041-1337/20/0000-00

DOI: 10.1097/TP.0000000000005138

INTRODUCTION

Kidney transplantation (KT) is challenged by the consistent shortage of kidneys from deceased donors. Recent research has indicated an independent association between deceased donor acute kidney injury (AKI), which is defined according to the AKI Network criteria,[1] and an increased likelihood of kidney discard, a tendency that shows a clear dependence on AKI stage.[2] Indeed, AKI in deceased donors implies a heightened risk of delayed graft function (DGF) in the short term[3]; however, its long-term impact on graft survival is debated. Furthermore, recent US registry data revealed no adverse effects on long-term graft survival because of AKI in deceased donors.[4,5] The strategy of using selected kidneys from deceased donors with AKI could potentially expand the availability of kidneys for transplantation. Therefore, it is crucial to develop a diagnostic tool that evaluates the presence and severity of AKI in deceased donor kidneys to prevent posttransplant renal dysfunction. Traditional biomarkers for the evaluation of kidney function, such as serum creatinine and cystatin C, are not sensitive or specific enough to diagnose AKI and do not correlate well with the severity of histological renal injury.[6-8] To date, suitable biomarkers for kidney injury are not yet fully understood (Figure 1A).

The kidney regulates endogenous hydrogen sulfide (H_2S) production.[9] H_2S is generated as a protector against tissue ischemia/reperfusion injury (IRI) via cystathionine-γ-lyase (CSE).[10-12] CSE mRNA expression has been reported to increase shortly after ischemia.[13] CSE is also responsible for the synthesis of cysteine, essential for the antioxidant defense system.[14] Cysteine is recognized as a biomarker for diseases because of its involvement in a wide range of mechanisms related to antioxidants, as it serves as one of the essential biothiols.[15-18]

Recently, we disclosed a fluorescent probe (NPO-B) that can selectively sense cysteine, which is high in glioblastoma tumor sites and urine samples from cervical cancer patients.[19,20] This probe can visualize and monitor cysteine levels in cells, tissue, and urine samples. To address the pressing need to augment

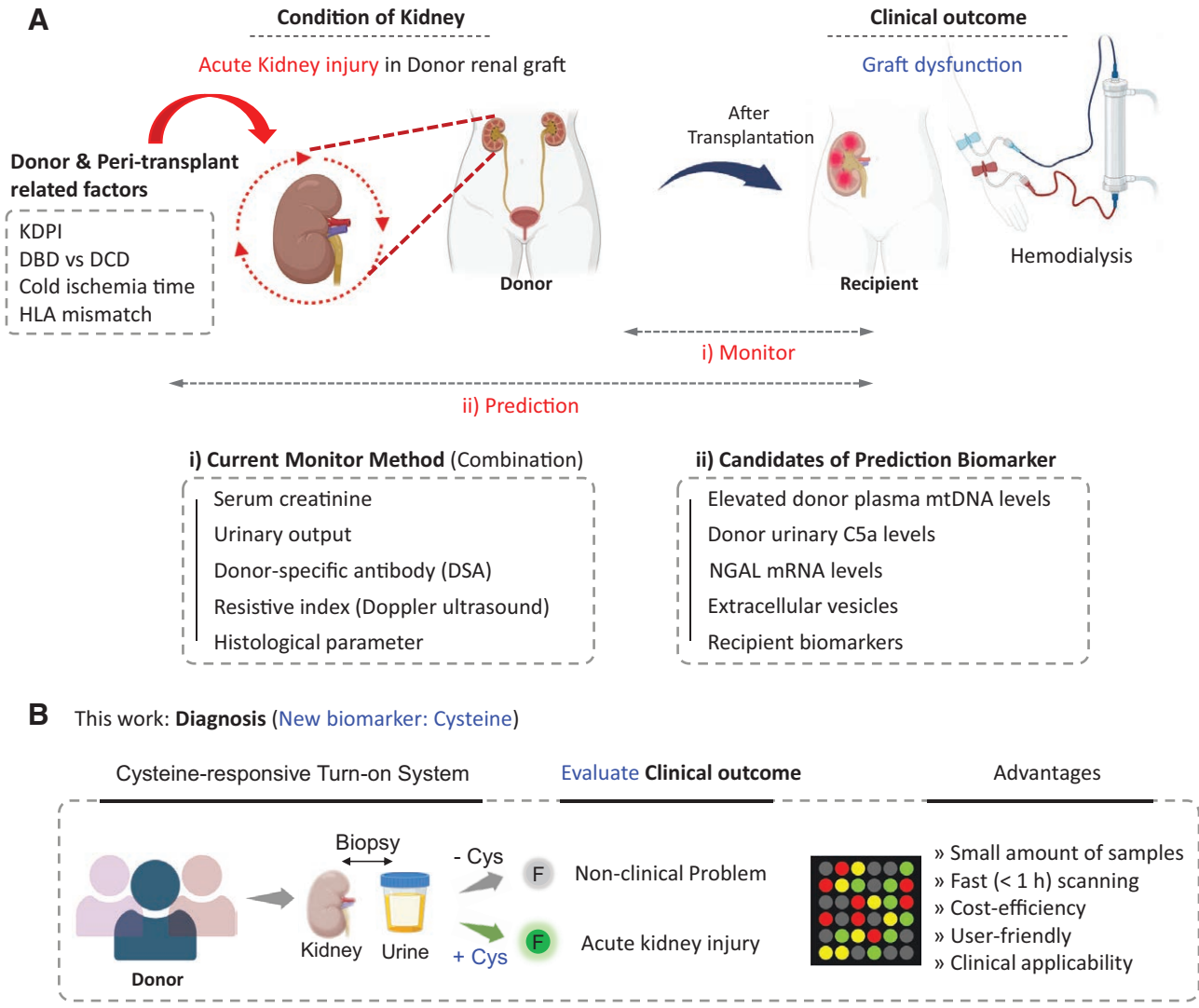

FIGURE 1. A schematic representation of the role of Cys as a diagnostic tool for kidney dysfunction after transplantation. A, Schematic drawing of the current monitoring method and potential biomarker candidates for predicting graft function after KT using donated renal grafts with AKI. B, A fluorescent molecular probe for the identification of kidney injury. The probe enables precise tracking of Cys levels in both kidney tissue and urine, thereby identifying Cys as a novel biomarker for AKI. AKI, acute kidney injury; Cys, cysteine; DBD, donation after brainstem death; DCD, donor after cardiac death; KDPI, Kidney Donor Profile Index; KT, kidney transplantation; NGAL, neutrophil gelatinase-associated lipocalin.

the pool of available kidneys for transplantation, we propose a new diagnostic model for kidney injury using cysteine and have verified its effectiveness (Figure 1B).

MATERIALS AND METHODS

Preparation and Identification of NPO-B

The structure of NPO-B, Smiles rearrangement-inspired cysteine-selective fluorescent probe, was verified using $^{1}H/^{19}F$-NMR, consistent with previous reports (**Figure S1, SDC,** http://links.lww.com/TP/D115).[19,20] Synthetic protocols and detailed information for reagents, instruments, and analytical methods can be found in **Supplemental Materials and Methods** (**SDC,** http://links.lww.com/TP/D115).

Cell Culture

Human kidney-2 (HK-2) cells (ATCC, CRL-2190; Manassas, VA) were cultured in DMEM/F12 (Life Technologies; Carlsbad, CA) supplemented with 10% fetal bovine serum (Life Technologies, Sydney, NSW, Australia) and 1% antibiotic/antimycotic in humidified atmosphere containing 95% air and 5% CO_2 at 37 °C, and the cells were subsequently subjected to hypoxia. For hypoxic preconditioning of the cells, they were incubated in a hypoxic chamber with 1% O_2 at 37 °C (**Supplemental Materials and Methods, SDC,** http://links.lww.com/TP/D115).

Quantitative analysis was performed using a Cysteine Assay Kit (Fluorometric) (ab211099). The assay principle is based on the cleavage of the thiol group in reduced cysteine to produce a signal that can be detected at excitation/emission = 365/450 nm. The intensity of the signal was directly proportional to the amount of total cysteine in the sample.

Fluorescence-based Analysis

The photophysical properties of the biological specimens (urine and plasma) were analyzed using NPO-B (concentration of 100 μM) with emission spectra recorded under fixed conditions (dark, scan speed: 6000 nm/min, slit: 3 nm/3 nm, 25 °C). To analyze the NPO-B reaction with or without cysteine, mouse/human urine and mouse plasma samples were incubated with cysteine (500 μM) at 37 °C for 30 min. The working concentration of NPO-B was 100 μM. The fluorescence intensity in mouse urine was measured at various concentrations of cysteine (range, 0.325–200 μM, with a 2-fold interval increment) after reaction with NPO-B. Additionally, fluorescence was measured over time (0–10 h, with 1 h intervals) after the reaction of NPO-B with cysteine at a 1:1 ratio at 37 °C.

To assess the specificity of NPO-B in detecting cysteine within the kidney, mouse kidneys were separately pretreated with either cysteine (500 μM) or cysteine (500 μM) + *N*-ethylmaleimide (NEM), scavenger of cysteine. After incubation for 1 h at 37 °C, the treated kidneys were washed 3 times with PBS. The kidneys were then treated with NPO-B solution in PBS (working concentration of NPO-B: 100 μM, PBS/dimethyl sulfoxide = 1:0.01) for 2 h in a shaking incubator at 37 °C, rewashed with PBS. Radiant efficiency across the kidney was measured under 400–450 nm excitation.

Two-photon microscopy (TPM) was used to visualize cysteine in the kidney with reduced tissue damage and low phototoxicity.[21-25] Kidneys were treated with NPO-B (100 μM) in PBS at 37 °C for 2 h for TPM-based monitoring of cysteine level.

For clinical feasibility purposes, the cold temperature resistance of the fluorescent probe was assessed. To confirm the reaction of NPO-B with cysteine at a cold temperature (4 °C), we conducted 2 analyses: (1) solution test and (2) tissue test. In the solution test, NPO-B (10 μM) was incubated with cysteine (50 μM) at 4 °C for 90 min. Then, the time-dependent fluorescent emission intensity was recorded every 30 min. In the tissue test, 3 mice were allocated to each group: the control group and the IRI-induced group induced by 45 min of ischemia and 24 h of reperfusion. After being stored in PBS at 4 °C for 5 h, extracted kidneys from both groups were immersed in a 4 °C NPO-B (100 μM) solution. Then, the entire kidney area was measured for its radiant efficiency.

Western Blot Analysis

Western blot analysis assessed the protein expression of CSE and hypoxia-inducible factor 1α in cell samples. The intensity of the protein bands was quantified using ImageJ software and normalized to the expression of the GAPDH. The detailed procedure can be found in **Supplemental Materials and Methods** (**SDC,** http://links.lww.com/TP/D115).

Animal Models

All mouse experiments followed the National Institutes of Health Guide for the Care and Use of Experimental Animals and were approved by the Animal Experimentation Ethics Committee of Seoul National University Hospital, Seoul, Korea (IACUC No. 21-0109-S1A1). BALB/c mice aged 7–9 wk purchased from ORIENT BIO, Korea, were randomly allocated into 3 groups: control group (n = 9), 20 min of ischemia (n = 16), and 45 min of ischemia (n = 16). For inducing IRI of the kidney, the left renal vascular pedicle was clamped for the designated time, and the animals were euthanized after a 24-h reperfusion period (**Supplemental Materials and Methods, SDC,** http://links.lww.com/TP/D115).

Kidney Histopathology and Immunohistochemistry

Paraformaldehyde-fixed kidneys were dehydrated using ethanol, embedded in paraffin, and sectioned to a thickness of 3 μm for light microscopy. Hematoxylin-eosin staining was performed to assess histological injury and fibrosis. The extent of apoptosis in the renal tissues was assessed using terminal deoxynucleotidyl transferase dUTP nick end labeling staining, performed using an ApopTag Red in Situ Apoptosis Detection Kit (Millipore, USA). The detailed methods for quantitative analysis are described in **Supplemental Materials and Methods** (**SDC,** http://links.lww.com/TP/D115).

Human Urine Samples

The single donor human urine (sex: male, age: 60s, race: White, condition: healthy, and code: IRHUURES50ML-27176) was purchased from Innovative Research Inc (MI) and used in the following studies: ultraviolet-visible and fluorescence analyses to measure the reaction with NPO-B and cysteine. The clinical urine

samples were collected from deceased kidney donors and living kidney donors from Seoul National University Hospital (Institutional Review Board No.: 2001-007-1091). Deceased donor urine was collected immediately before aorta cross-clamping.

Statistical Analysis

The data are expressed as the mean ± SEM unless otherwise stated. Statistical comparisons were performed using 2-way ANOVA.

For all tests, significance is defined as $^{****}P < 0.0001$, $^{***}P < 0.001$, $^{**}P < 0.01$, and $^{*}P < 0.05$. Differences were considered statistically significant at P values <0.05. Statistical tests were performed using IBM SPSS version 26 (IBM Inc, Chicago, IL) and GraphPad InStat version 5.01 (GraphPad Software, La Jolla, CA).

RESULTS

NPO-B Identification

It is well known that cysteine levels rise in hypoxic conditions to combat reactive oxygen species.[26] Hence, we hypothesized that elevated cysteine levels in urine and tissue samples because of brain death and hemodynamic instability could indicate kidney injury and be detected by NPO-B (Figure 2A). The NPO-B probe, containing an arene moiety with penta-fluoro, selectively detects cysteine over homocysteine (Hcy) and glutathione (GSH) via Smile

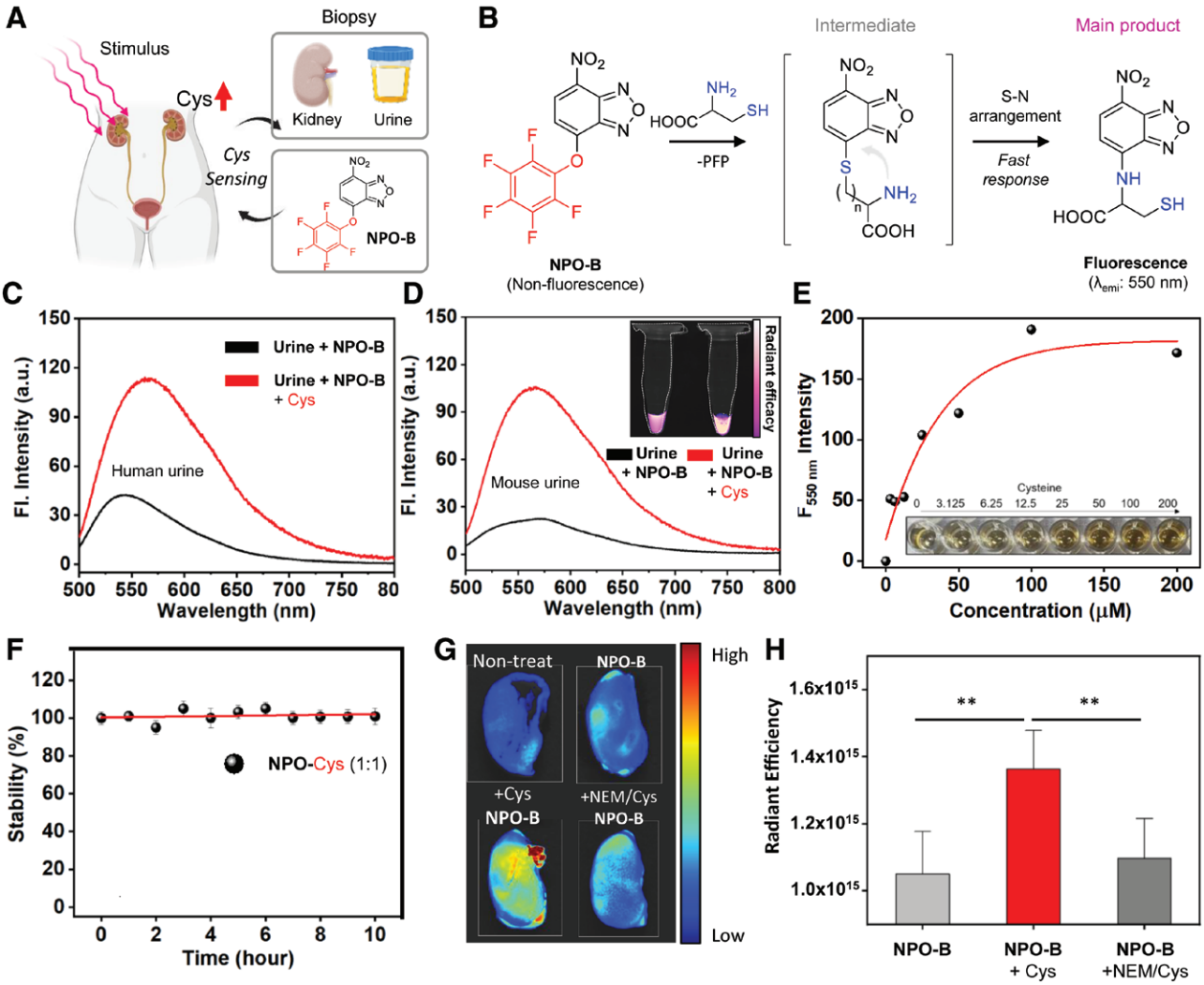

FIGURE 2. NPO-B characterization for Cys in normal urine and normal kidney. A, Schematic illustration of the Cys sensing rationale by internal/external stimulation using NPO-B in normal urine and normal kidney. B, Cys sensing mechanism (turn-on) using NPO-B. The sensing mechanism was based on the Smile rearrangement reaction and an electron-density approach of the arene moiety. C, Emission spectra of NPO-B (100 μM) with/without Cys (5 eq) in human normal urine (sex: male, age: 60s, race: White, condition: healthy, and code: IRHUURES50ML-27176). D, Emission spectra of NPO-B (100 μM) with/without Cys in mouse urine (BALB/c, 7–9 wk). Inserted image: fluorescent image under a radiant efficiency value (C and D) was measured after incubation with Cys (500 μM; 5 eq) at 37 °C for 30 min. E, The FI plot of NPO-B is dependent on the concentration of Cys (0.325–200 μM, interval increment: 2-fold) in mouse urine. Inserted image: naked image under white light, left to right: increased concentration of Cys in urine. F, Fluorescence intensity plot of NPO-Cys (after reaction of NPO-B and Cys; 1:1) dependent on time (0 to 10 h, interval time: 1 h, incubation temperature: 37 °C). G, FTIS image of normal mouse kidney (BALB/c, 7–9 wk) with pretreatment of Cys alone (500 μM) and NEM (500 μM) + Cys (500 μM, treated after pretreatment of NEM). NPO-B (100 μM) was incubated for 2 h at 37 °C. H, Radiant efficiency plot from panel G. The error bar represents mean ± SD (n = 3) with 1-way ANOVA and Tukey multiple comparison tests; $^{**}P < 0.01$. Cys, Cys, cysteine; FI, fluorescence intensity; FTIS, fluorescence tissue imaging system; NEM, *N*-ethylmaleimide.

rearrangement in aqueous solution. After the reaction of NPO-B with cysteine, fluorescence was turned on at a maximum wavelength of 550 nm (Figure 2B). We observed that the emission intensity of the reaction result of NPO-B with cysteine could surpass the autofluorescence in human/mouse urine (Figure 2C and D), whereas in mouse plasma, the emission spectra showed no significant changes even with the addition of cysteine (**Figure S2, SDC,** http://links.lww.com/TP/D115). Additionally, NPO-B exhibited strong sensitivity toward cysteine with concentration-dependent response curves ranging from 0.325 to 200 μM in normal mouse urine (Figure 2E). Therefore, urine was selected as the monitoring material for kidney injury. The fluorescent stability of the reaction product (NPO-cysteine) was evaluated, and the fluorescent intensity at 550 nm remained consistent (Figure 2F). To confirm whether cysteine within the kidney can be imaged, we added extra cysteine by soaking the kidney in cysteine solution (pH 7.4) for 1 h. Another group was pretreated with NEM for 1 h using the same process. The fluorescence tissue imaging system (FTIS) image showed enhanced fluorescence in cysteine-soaked kidneys, whereas the NEM-pretreated group showed no change even with cysteine addition (Figure 2G and H). Given the successful detection of cysteine in human and mouse urine and kidneys using NPO-B, we further investigated the effect of hypoxia and reoxygenation on cellular cysteine levels.

Analysis of CSE Expression and Cysteine Levels in HK-2 Cells

We hypothesized that NPO-B could react with the increased intracellular cysteine induced by overexpressed CSE to maintain homeostasis after hypoxia-reoxygenation injury (Figure 3A). We analyzed CSE expression in HK-2 cells under hypoxia-reoxygenation injury. Western blot analysis showed a significant rise in CSE and hypoxia-inducible factor 1α levels in HK-2 cells under 24-h hypoxia compared with controls ($^{*}P < 0.05$ and $^{**}P < 0.01$; Figure 3B and C). In the quantitative analysis performed to measure intracellular cysteine at different time points (6–48 h) under hypoxic conditions (1.0% O_2), followed by 24 h of reoxygenation, cysteine levels were significantly higher after hypoxia ($^{***}P < 0.001$; Figure 3D). Confocal microscopy images of HK-2 cells treated with NPO-B (concentration: 5 μM, incubation: 15 min) with or without hypoxia-induced stress (hypoxia

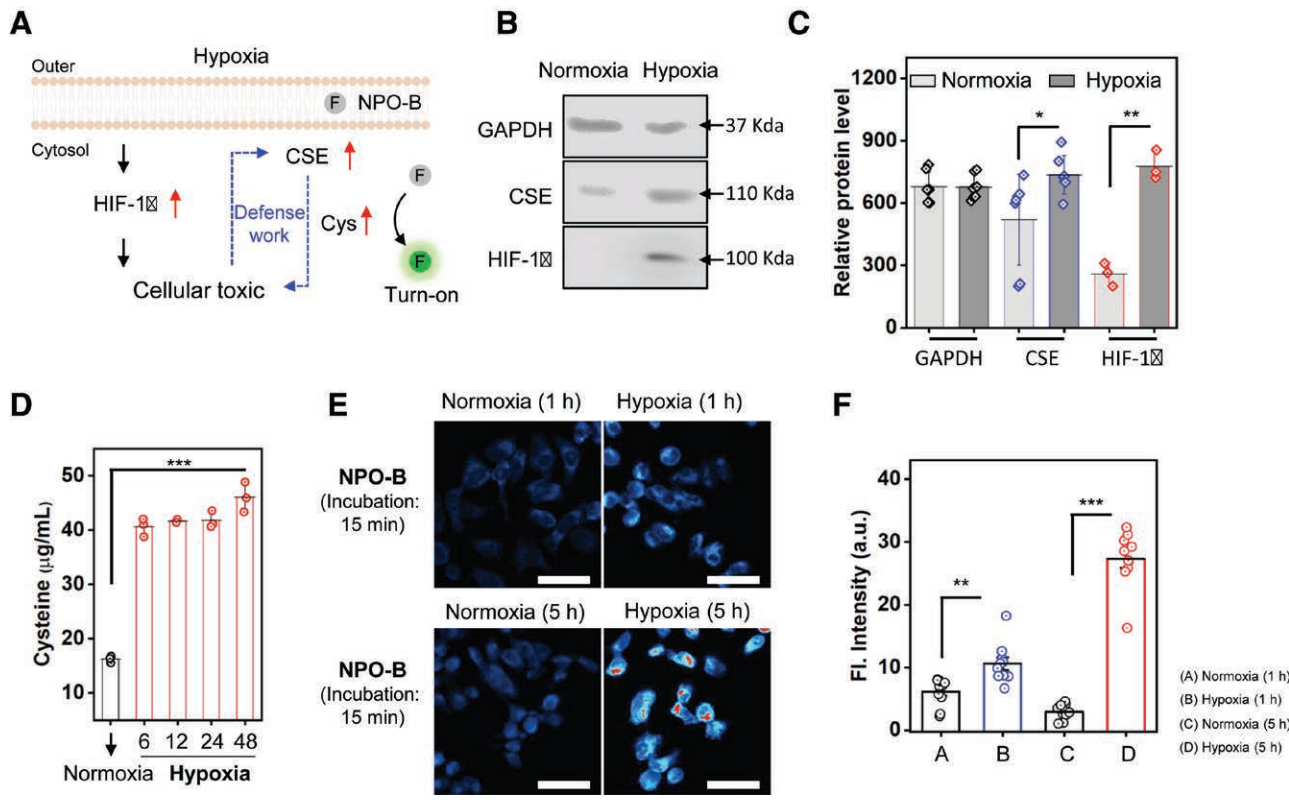

FIGURE 3. In vitro HK-2 cell analysis using NPO-B under external stimulation (hypoxia-induced stress). A, Schematic illustration of homeostasis of intracellular cysteine by hypoxia and sensing strategy using NPO-B (marked as F). B, Western blot analysis using HK-2 cells after hypoxia-induced stress for 24 h (hypoxia condition: 1% O_2). GAPDH was probed as a loading control. C, Quantitative protein level analysis using panel B. The error bar represents mean ± SEM (n = 6) with an unpaired *t* test (comparison between normoxia and hypoxia); $^{*}P < 0.05$ (CSE), $^{**}P < 0.01$ (hypoxia). The dot plots represent jitter points. D, Quantitative analysis of intracellular Cys dependent on hypoxia-induced time (6–48 h, hypoxia condition: 1% O_2). The error bar represents mean ± SEM (n = 3) with 1-way ANOVA and Tukey multiple comparison tests; normoxia vs hypoxia (6, 12, 24, and 48 h, respectively): $^{***}P < 0.001$. The dot plots represent jitter points. E, confocal microscope images after treatment of NPO-B (concentration: 5 μM, incubation: 15 min) in HK-2 cells with/without hypoxia-induced stress (hypoxia time: 1 h and 5 h). The color was replaced by an artificial cyanine gradient color (blue to red means low to high intensity). F, Fluorescent intensity plot using the panel E image. The entire cellular membrane was delineated using Image J software, leveraging a blinded fluorescence image. The error bar represents mean ± SEM with 1-way ANOVA and Tukey multiple comparison tests; $^{**}P < 0.001$ (A vs B), $^{***}P < 0.001$ (C vs D). The dot plots represent jitter points. CSE, cystathionine gamma-lyase; Cys, cysteine; FI, fluorescence intensity; HIF-1α, hypoxia-inducible factor 1-alpha; HK-2, human kidney-2.

time: 1 and 5 h) showed increased fluorescence after hypoxia (Figure 3E; **Figures S3 and S4, SDC,** http://links.lww.com/TP/D115). Fluorescence intensities at 1 and 5 h after hypoxia were significantly higher than those under normoxic conditions (**$P < 0.01$, ***$P < 0.001$; Figure 3F).

In Vivo Visualization of Injured Kidneys Using NPO-B

Mice in the IRI group underwent left renal ischemia, followed by 24 h of reperfusion. After intravenous injection of NPO-B (5 mpk) through the tail vein, the organs were procured after 30, 120, and 240 min and analyzed using FTIS (390–490 nm excitation, 500–550 nm detection channel). We also soaked IRI mouse kidneys in the NPO-B (100 μM) solution for 2 h at 37 °C (Figure 4A).

As shown in **Figure S5** (**SDC,** http://links.lww.com/TP/D115), H&E-stained sections revealed severe tubular interstitial damage in IRI mouse kidneys, more pronounced in the 45 min IRI group (**Figure S5A, SDC,** http://links.lww.com/TP/D115). Terminal deoxynucleotidyl transferase dUTP nick end labeling assay showed increased apoptosis in IRI kidney tissues (**Figure S5A, SDC,** http://links.lww.com/

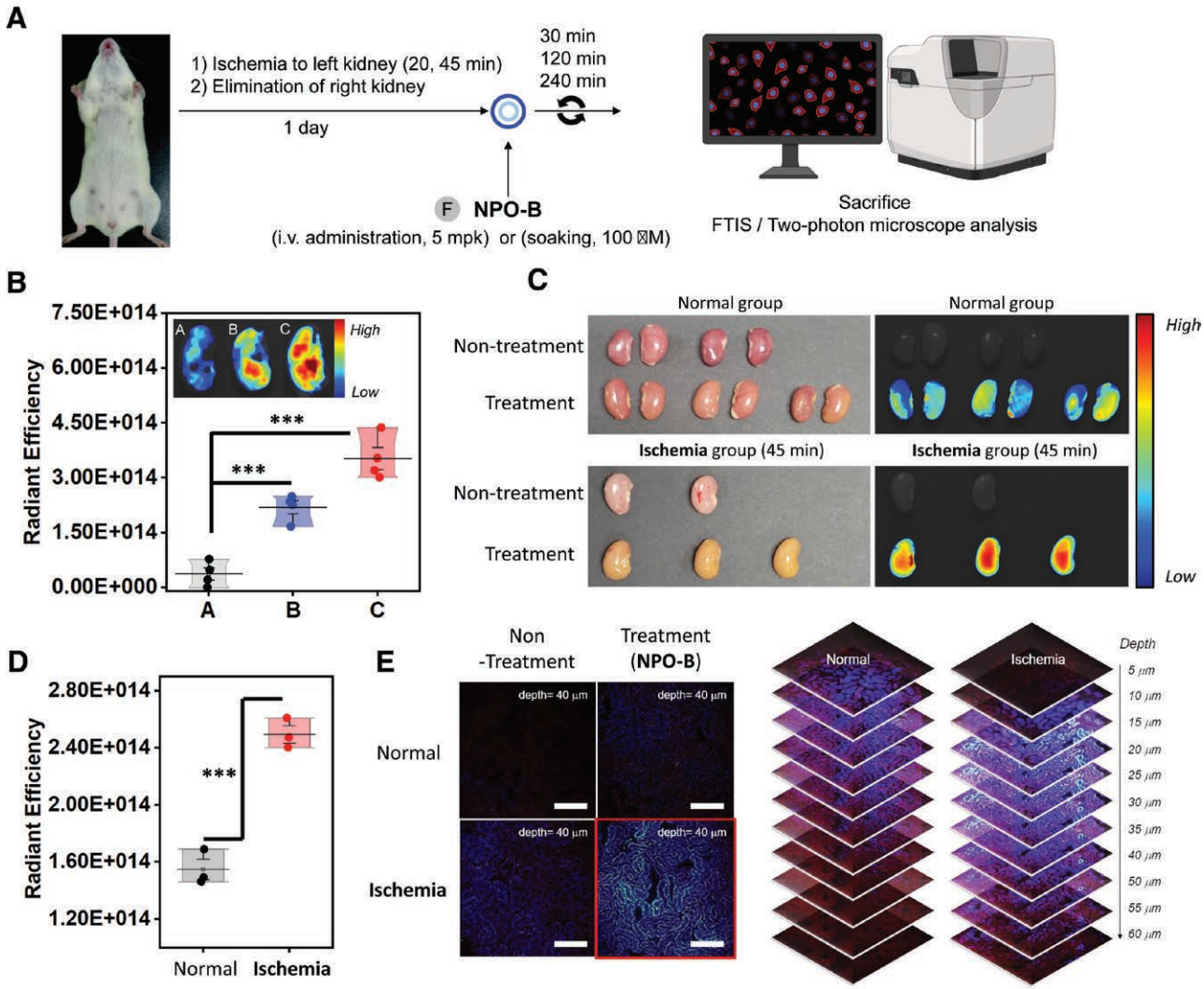

FIGURE 4. In vivo/ex vivo kidney analysis using NPO-B under external stimulation (IRI-induced stress). A, The entire procedure for in vivo analysis using NPO-B. External stimulation by I/R was performed. The I/R was conducted in the left kidney (BALB/c, 7–9 wk). A concentration of 5 mpk (mg/kg) of NPO-B was administered via tail-vein injection, whereas a soaking test used a concentration of 100 μM of NPO-B. The time points analyzed were 30, 120, and 240 min, respectively. The ischemia was induced by clamping the left renal artery/vein for 20 and 45 min, respectively. The analysis was performed by 2 methods. B, The radiant efficiency plot after administration of NPO-B (5 mpk) into tail vein with 240 min duration of NPO-B circulation. A, Normal group; B, I/R group (Ischemia 20 min); C, I/R group (ischemia 45 min). The error bar represents mean ± SEM (n = 4) with 1-way ANOVA and Tukey multiple comparison tests; a range of percentage was shown as 10, 25, 75, and 90 (coefficient = 1); $P = 0.0006$ (***), t (df) = 9.966. C, Soaking analysis image after incubation of kidney (normal vs I/R (ischemia: 45 min)) with NPO-B (100 μM). The FTIS data were obtained under excitation at 488 nm. The fluorescent intensity was expressed by radiant efficiency. D, The radiant efficiency plot was obtained from the soaking analysis after incubation of the kidney (normal vs ischemia) with NPO-B. The error bar represents mean ± SEM (n = 3) with an unpaired t test (2-tailed); a range of percentages was shown as 10, 25, 75, and 90 (coefficient = 1). Whisker values for the analysis of the normal group were 1.4745×10^{14} and 1.16189×10^{14}, respectively. Whisker values for the ischemia group were 2.4316×10^{14} and 2.5551×10^{14}, respectively; P value = 0.0006 (***), t (df) = 9.966. E, TP microscopy analysis after soaking of the kidney (normal or IRI-induced stress) into NPO-B. Left: cross-sectional image (depth: 40 μm from the central surface of the kidney). Right: cross-sectional stack image of both normal and the I/R (ischemia: 45 min) groups. FTIS, fluorescence tissue imaging system; I/R, ischemia-reperfusion; IRI, I/R injury; TP, 2-photon.

TP/D115). Tubular injury scores were higher in IRI groups, especially in the 45-min IRI group than in the 20-min IRI group (**Figure S5B, SDC,** http://links.lww.com/TP/D115). Apoptotic cell counts increased with ischemia time. These findings confirm that the kidney sustains damage because of IRI, and the extent of damage is dependent on the duration of ischemia. Next, we analyzed the circulation time (30, 120, and 240 min) of NPO-B after administration of NPO-B (5 mpk) into the tail vein of IRI mice. As shown in Figure 4B and **Figure S6** (**SDC,** http://links.lww.com/TP/D115), the IRI kidney (20 and 45 min) exhibited an observable trend of increased radiant efficiency, which was influenced by the duration of circulation (30 and 240 min), with a particularly significant increase at 240 min (***$P < 0.001$; Figure 4B). These results indicate the 240 min circulation of NPO-B in vivo effectively evaluates IRI kidneys. The autofluorescence effect in both normal and IRI kidneys after treatment with PBS was minimal (**Figure S7, SDC,** http://links.lww.com/TP/D115).

As a simpler and noninvasive method, kidneys were soaked in NPO-B (100 μM) for 2 h and then rinsed after 45 min of ischemia and 24 h of reperfusion. Fluorescence signals were stronger in the kidneys incubated with NPO-B than in controls, as shown by FTIS analysis (Figure 4C and D). Both results (injection and soaking methods) demonstrated a higher distribution of cysteine within injured kidneys than in normal kidneys. In the TPM analysis performed to clarify this further, strong fluorescence was observed in the kidney tissues of IRI mice compared with the control group when excited at 900 nm (Figure 4E, left). In z-stacked TPM images of each kidney sample with NPO-B, the signal was the brightest in the zone 40 μm from the surface, indicating high permeability NPO-B (Figure 4E, right).

In the evaluation of the cold temperature resistance of the fluorescent probe, unlike the 37 °C condition, the reaction of NPO-B with cysteine continued for up to 90 min at the 4 °C condition (**Figure S8, SDC,** http://links.lww.com/TP/D115). However, the fluorescence intensity was strong enough to detect the cysteine in cold solution. We also performed the IRI-induced kidney analysis using a soaking method at cold conditions (4 °C; **Figure S9**, **SDC,** http://links.lww.com/TP/D115). The visualization of the IRI-induced kidney significantly discriminated against the normal group, indicating that the cold storage did not affect the probe's reaction ability.

Analysis of Mouse/Human Urine Samples Using NPO-B

Given that NPO-B shows promising properties of urinalysis without autofluorescence (Figure 2) and visualization of the hypoxia-induced kidney cell line (Figure 3) and IRI kidney (Figure 4), we sought to measure cysteine in urine obtained from kidney donors using NPO-B. Our objective was to evaluate kidney injury in deceased donors who are at a high risk of renal injury because of various risk factors. Deceased donors can lead to poor outcomes, including DGF for recipients after KT. Initially, we aimed to verify whether urine cysteine exhibited similar trends to commonly used markers for AKI, such as blood urea nitrogen, serum creatinine, and urinary neutrophil gelatinase-associated lipocalin (uNGAL).[27,28] As seen in Figure 5A–C, blood urea nitrogen, serum creatinine, and uNGAL showed a progressive increase corresponding to the duration of ischemia (20 and 45 min) in mice. The emission intensity of NPO-B at 550 nm increased with the duration of ischemia (20 and 45 min), suggesting that urinary cysteine could be a new biomarker and NPO-B could be a promising tool to predict AKI (Figure 5D). Next, we applied this detection technique to humans. We compared urine samples from 91 deceased donors to those from 309 living donors. Considering that deceased donors often experience severe AKI and living donors could serve as healthy controls, our intention was to assess the extent of kidney injury in deceased donors by detecting cysteine levels in their respective urine samples. After incubating the urine samples with NPO-B for 40 min, we observed highly increased emission spectra (red line) in the deceased donor group compared with the living donor group (**Figure S10, SDC,** http://links.lww.com/TP/D115). We measured the fluorescence intensities of urine in both groups using NPO-B and found that the fluorescence intensity of urine from the deceased donors was significantly stronger than that of the living donors (***$P < 0.001$; Figure 5E).

DISCUSSION

KT offers better survival and cost-effectiveness for end-stage renal disease patients than maintenance dialysis and reduces cardiovascular mortality.[29-31] Yet, many donated kidneys are discarded, especially because of AKI, which is prevalent in deceased donors. Deceased organ donors can develop AKI in the setting of brain or circulatory death owing to significant hemodynamic changes or intrinsic tissue injury.[32-34] In fact, the discard rate was 30% for donors with AKI compared with 18% for donors without AKI, increasing with the severity of AKI.[2,35] However, recent findings suggest that donor kidneys with AKI can yield satisfactory outcomes.[36] As the list of transplant recipients steadily increases, the necessity to broaden the donor pool has emerged, leading to the acceptance of "less-than-ideal" kidneys. Although kidneys from AKI donors may experience DGF, long-term results can be comparable with those from non-AKI donors. Hence, detecting AKI biomarkers in donor kidneys becomes paramount for recipient risk stratification, quick AKI diagnosis, and potentially widening the donor pool. Previous experimental and clinical models have shown that uNGAL, urinary kidney injury molecule-1, and urinary interleukin-18 are specific markers of AKI and IRI,[37,38] and miR-182-5p and miR-21-3p emerge as promising DGF biomarkers after KT.[39] However, their practical application remains uncertain because many findings come from mouse studies, questioning their relevance in humans.

Cysteine, the most abundant in plasma, is a key oxidative stress marker. Several cysteine detection techniques, such as potentiometry, colorimetry, and high-performance liquid chromatography, face challenges such as complexity, high costs, and lengthy processes.[40-42] Despite numerous reported fluorescent-based biothiol probes, few accurately detect cysteine over Hcy and GSH, primarily tested in vitro. We developed NPO-B, operating on a Smile rearrangement mechanism, which is a turn-on mechanism providing a faster response to cysteine than Hcy and GSH. Unlike conventional detection tools, the NPO-B probe accurately detects cysteine both in 37 °C conditions and in cold solutions as well as cold preserved kidneys. This

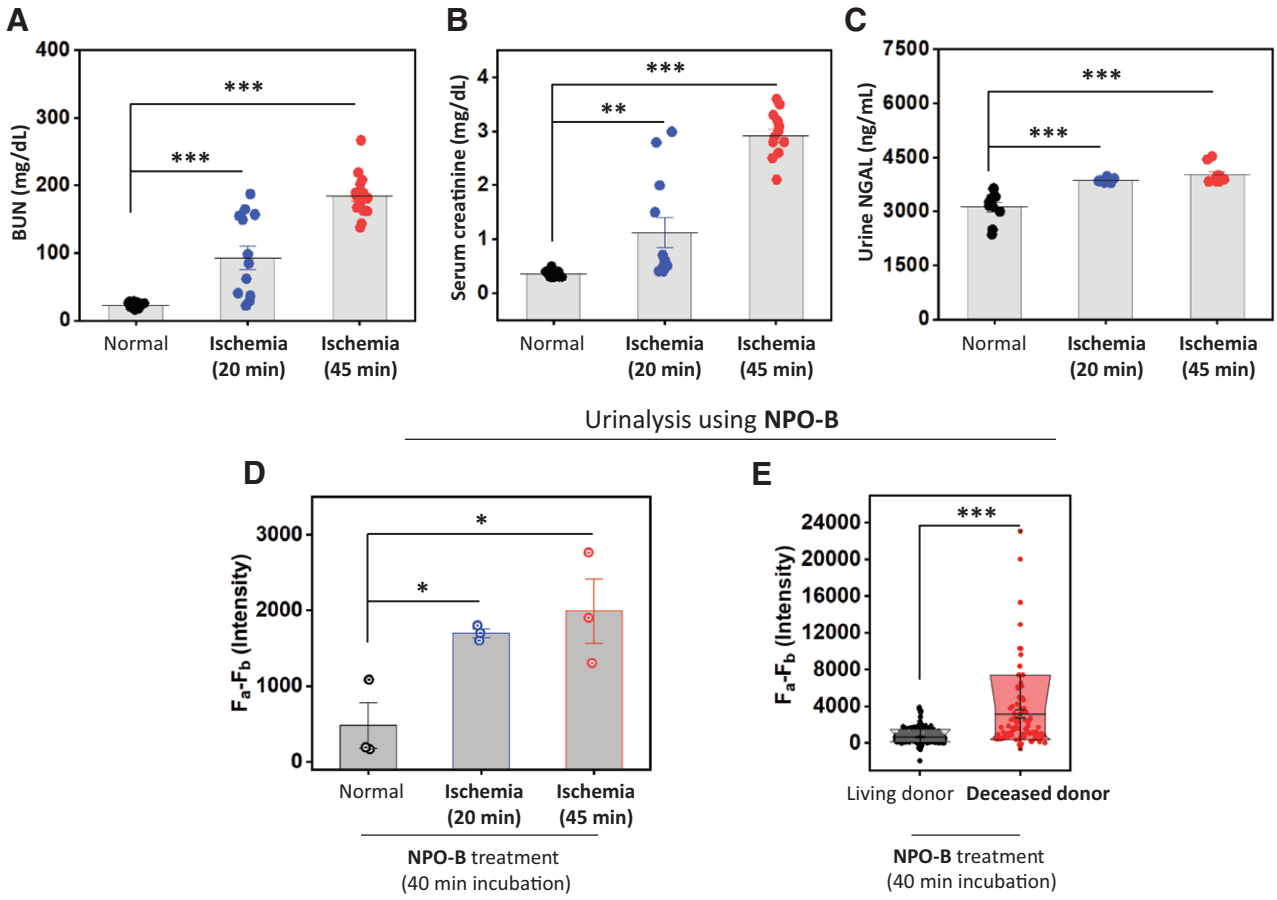

FIGURE 5. Analysis of urines from an IRI-induced mouse and deceased donors. A–C, A standard marker indicating damaged kidney (BUN, serum creatinine, NGAL). D, IRI-induced mouse urinalysis using NPO-B (concentration: 100 μM, incubation: 40 min). F_a = emission intensity at 550 nm after reaction, F_b = emission intensity at 550 nm before reaction. The error bar represents mean ± SEM with 1-way ANOVA and Tukey multiple comparison tests; $^*P < 0.05$. The dot plots represent jitter points. E, The emission intensity plot analysis at 550 nm. The data were obtained from **Figure S10** (**SDC,** http://links.lww.com/TP/D115). BUN, blood urea nitrogen; IRI, ischemia/reperfusion injury; NGAL, neutrophil gelatinase-associated lipocalin.

highlights the potential for NPO-B to be used in clinical settings. Compared with conventional monitoring methods, this approach has several strengths, including a low risk of clinical complications, the ability to make accurate predictions with a small sample size, rapid results obtainable within 1 h, and cost-effectiveness. Moreover, because of its less invasive and time-consuming nature compared with procurement biopsies, cysteine detection with NPO-B could be a promising tool to evaluate the degree of kidney injury in clinical transplantation.

We recently reported the utility of NPO-B in detecting cysteine in urine for cervical cancer diagnosis.[20] This suggests that increased cysteine in the urine of deceased donors may originate not only from renal cells but also from other cell types. Indeed, cysteine has been recognized as a biomarker for diseases such as neurological disorders, epilepsy, and various types of cancer.[18] However, considering the elevated intensity identified in the kidney and urine of IR-injured mice, cysteine, as a major indicator of oxidative stress, can serve at least as a complementary biomarker, enhancing the identification of renal injury when combined with other markers indicative of renal injury.

Kidneys obtained from deceased donors, especially high-risk donors, are associated with an increased incidence of DGF after KT,[43-46] and the degree of acute and chronic injuries in donor kidney varies based on the characteristics of the deceased donor.[47] As DGF adversely impacts both short- and long-term transplant outcomes, accurate evaluation of the donor is crucial. Previous studies have established numerous donor assessments, and significant efforts have been made to develop a reliable clinical prediction model.[47-50] However, the predictive power of various developed DGF prediction models remains limited, with area under the receiver operating characteristic curve ranging from 0.5 to 0.73.[51-56] Although the KDRI scoring system offers a preoperative prediction of DGF,[57] it does not account for other factors, such as cold ischemic time, immune status, and other relevant variables contributing to the risk of DGF. Based on the results of this study, urine cysteine level appears to be useful not only for evaluating kidney injury but also for predicting DGF. Although the urine samples collected from deceased donors in this study were insufficient to construct an actual DGF prediction model, integrating urine cysteine levels into existing prediction models is expected to enhance their prediction accuracy.

This study has several limitations. First, the sample size of deceased donors was small for constructing a definitive predictive model for DGF, as mentioned earlier. However, in Korea, collecting deceased donors' samples requires family consent, and this is currently

not performed in organ procurement organizations. Therefore, using urinary cysteine levels from deceased donors is difficult without international collaboration. Second, the retrospective study design limited control over variables such as food and medication and potentially effective urinary cysteine levels. Moreover, the lack of fresh tissue storage in our biobank prevented direct visualization of cysteine with NPO-B in fixed deceased donor kidney tissues. Fixative solutions such as formaldehyde are widely acknowledged to react with various amino acids, particularly cysteine, forming hemithioacetal and thiazolidine products.[58] This limitation is inherent in retrospective studies and, therefore, emphasizes the necessity of using fresh tissue in future studies to accurately investigate the interaction of NPO-B with cysteine in deceased donors. Finally, assessing the long-term effects of elevated urinary cysteine levels on graft outcomes is crucial, as predicting long-term graft outcomes remains challenging.[59-62] Large-scale, long-term follow-up studies are warranted to improve the clinical utility of NPO-B in transplantation.

In conclusion, we verified the efficacy of a fluorescent cysteine probe for detecting cysteine in urine and kidney tissue. We anticipate that our diagnostic method can improve KT outcomes by accurately identifying damage to the pretransplant kidney graft.

ACKNOWLEDGMENTS

The authors thank Sangwan Kim for providing statistical support.

REFERENCES

1. Mehta RL, Kellum JA, Shah SV, et al; Acute Kidney Injury Network. Acute kidney injury network: report of an initiative to improve outcomes in acute kidney injury. *Crit Care*. 2007;11:R31.
2. Hall IE, Schroppel B, Doshi MD, et al. Associations of deceased donor kidney injury with kidney discard and function after transplantation. *Am J Transplant*. 2015;15:1623–1631.
3. Zheng YT, Chen CB, Yuan XP, et al. Impact of acute kidney injury in donors on renal graft survival: a systematic review and meta-analysis. *Ren Fail*. 2018;40:649–656.
4. Hall IE, Akalin E, Bromberg JS, et al. Deceased-donor acute kidney injury is not associated with kidney allograft failure. *Kidney Int*. 2019;95:199–209.
5. Liu C, Hall IE, Mansour S, et al. Association of deceased donor acute kidney injury with recipient graft survival. *JAMA Netw Open*. 2020;3:e1918634.
6. Koyner JL, Garg AX, Coca SG, et al; TRIBE-AKI Consortium. Biomarkers predict progression of acute kidney injury after cardiac surgery. *J Am Soc Nephrol*. 2012;23:905–914.
7. Koyner JL, Parikh CR. Clinical utility of biomarkers of AKI in cardiac surgery and critical illness. *Clin J Am Soc Nephrol*. 2013;8:1034–1042.
8. Moledina DG, Hall IE, Thiessen-Philbrook H, et al. Performance of serum creatinine and kidney injury biomarkers for diagnosing histologic acute tubular injury. *Am J Kidney Dis*. 2017;70:807–816.
9. Han Y, Shang Q, Yao J, et al. Hydrogen sulfide: a gaseous signaling molecule modulates tissue homeostasis: Implications in ophthalmic diseases. *Cell Death Dis*. 2019;10:293.
10. House JD, Brosnan ME, Brosnan JT. Characterization of homocysteine metabolism in the rat kidney. *Biochem J*. 1997;328(Pt 1):287–292.
11. Prathapasinghe GA, Siow YL, O K. Detrimental role of homocysteine in renal ischemia-reperfusion injury. *Am J Physiol Renal Physiol*. 2007;292:F1354–F1363.
12. Xu Z, Prathapasinghe G, Wu N, et al. Ischemia-reperfusion reduces cystathionine-beta-synthase-mediated hydrogen sulfide generation in the kidney. *Am J Physiol Renal Physiol*. 2009;297:F27–F35.
13. Bos EM, Wang R, Snijder PM, et al. Cystathionine gamma-lyase protects against renal ischemia/reperfusion by modulating oxidative stress. *J Am Soc Nephrol*. 2013;24:759–770.
14. Paul BD, Snyder SH. H(2)S signalling through protein sulfhydration and beyond. *Nat Rev Mol Cell Biol*. 2012;13:499–507.
15. Chen X, Zhou Y, Peng X, et al. Fluorescent and colorimetric probes for detection of thiols. *Chem Soc Rev*. 2010;39:2120–2135.
16. Ulrich K, Jakob U. The role of thiols in antioxidant systems. *Free Radic Biol Med*. 2019;140:14–27.
17. Paulsen CE, Carroll KS. Cysteine-mediated redox signaling: chemistry, biology, and tools for discovery. *Chem Rev*. 2013;113:4633–4679.
18. Rehman T, Shabbir MA, Inam-Ur-Raheem M, et al. Cysteine and homocysteine as biomarker of various diseases. *Food Sci Nutr*. 2020;8:4696–4707.
19. An JM, Kang S, Huh E, et al. Penta-fluorophenol: a Smiles rearrangement-inspired cysteine-selective fluorescent probe for imaging of human glioblastoma. *Chem Sci*. 2020;11:5658–5668.
20. An JM, Suh J, Kim J, et al. First-in-class: cervical cancer diagnosis based on a urine test with fluorescent cysteine probe. *Sens Actuators B Chem*. 2022;360:131646.
21. Helmchen F, Denk W. Deep tissue two-photon microscopy. *Nat Methods*. 2005;2:932–940.
22. Nwaneshiudu A, Kuschal C, Sakamoto FH, et al. Introduction to confocal microscopy. *J Invest Dermatol*. 2012;132:e3.
23. Yew E, Rowlands C, So PT. Application of multiphoton microscopy in dermatological studies: a mini-review. *J Innov Opt Health Sci*. 2014;7:1330010.
24. Konig K. Multiphoton microscopy in life sciences. *J Microsc*. 2000;200(Pt 2):83–104.
25. Weigert R, Sramkova M, Parente L, et al. Intravital microscopy: a novel tool to study cell biology in living animals. *Histochem Cell Biol*. 2010;133:481–491.
26. Nunes SC, Ramos C, Lopes-Coelho F, et al. Cysteine allows ovarian cancer cells to adapt to hypoxia and to escape from carboplatin cytotoxicity. *Sci Rep*. 2018;8:9513.
27. Hou J, Tolbert E, Birkenbach M, et al. Treprostinil alleviates hepatic mitochondrial injury during rat renal ischemia-reperfusion injury. *Biomed Pharmacother*. 2021;143:112172.
28. Monari E, Troìa R, Magna L, et al. Urine neutrophil gelatinase-associated lipocalin to diagnose and characterize acute kidney injury in dogs. *J Vet Intern Med*. 2020;34:176–185.
29. Wolfe RA, Ashby VB, Milford EL, et al. Comparison of mortality in all patients on dialysis, patients on dialysis awaiting transplantation, and recipients of a first cadaveric transplant. *N Engl J Med*. 1999;341:1725–1730.
30. Meier-Kriesche HU, Schold JD, Srinivas TR, et al. Kidney transplantation halts cardiovascular disease progression in patients with end-stage renal disease. *Am J Transplant*. 2004;4:1662–1668.
31. Yang F, Liao M, Wang P, et al. The cost-effectiveness of kidney replacement therapy modalities: a systematic review of full economic evaluations. *Appl Health Econ Health Policy*. 2021;19:163–180.
32. Davenport A. The brain and the kidney—organ cross talk and interactions. *Blood Purif*. 2008;26:526–536.
33. Wu VC, Wu PC, Wu CH, et al; National Taiwan University Study Group on Acute Renal Failure (NSARF) Group. The impact of acute kidney injury on the long-term risk of stroke. *J Am Heart Assoc*. 2014;3:e000933.
34. Reese PP, Doshi MD, Hall IE, et al. Deceased-donor acute kidney injury and acute rejection in kidney transplant recipients: a multicenter cohort. *Am J Kidney Dis*. 2023;81:222–231.e1.
35. Koyawala N, Parikh CR. A review of donor acute kidney injury and posttransplant outcomes. *Transplantation*. 2020;104:1553–1559.
36. Heilman RL, Smith ML, Smith BH, et al. Long-term outcomes following kidney transplantation from donors with acute kidney injury. *Transplantation*. 2019;103:e263–e272.
37. Haase M, Bellomo R, Devarajan P, et al; NGAL Meta-analysis Investigator Group. Accuracy of neutrophil gelatinase-associated lipocalin (NGAL) in diagnosis and prognosis in acute kidney injury: a systematic review and meta-analysis. *Am J Kidney Dis*. 2009;54:1012–1024.
38. Siew ED, Ware LB, Ikizler TA. Biological markers of acute kidney injury. *J Am Soc Nephrol*. 2011;22:810–820.
39. Wilflingseder J, Sunzenauer J, Toronyi E, et al. Molecular pathogenesis of post-transplant acute kidney injury: assessment of whole-genome mRNA and miRNA profiles. *PLoS One*. 2014;9:e104164.
40. Adamo M, Sun G, Qiu D, et al. Drug-to-antibody determination for an antibody-drug-conjugate utilizing cathepsin B digestion coupled

with reversed-phase high-pressure liquid chromatography analysis. *J Chromatogr A*. 2017;1481:44–52.
41. Kim CJ, Lee DI, Kim C, et al. Gold nanoparticles-based colorimetric assay for cathepsin B activity and the efficiency of its inhibitors. *Anal Chem*. 2014;86:3825–3833.
42. Song Y, Fan H, Anderson MJ, et al. Electrochemical activity assay for protease analysis using carbon nanofiber nanoelectrode arrays. *Anal Chem*. 2019;91:3971–3979.
43. Siedlecki A, Irish W, Brennan DC. Delayed graft function in the kidney transplant. *Am J Transplant*. 2011;11:2279–2296.
44. Zens TJ, Danobeitia JS, Leverson G, et al. The impact of kidney donor profile index on delayed graft function and transplant outcomes: a single-center analysis. *Clin Transplant*. 2018;32:13190.
45. Xue W, Tian P, Xiang H, et al. Outcomes for primary kidney transplantation from donation after citizens' death in China: a single center experience of 367 cases. *BMC Health Serv Res*. 2017;17:250.
46. Chaumont M, Racapé J, Broeders N, et al. Delayed graft function in kidney transplants: time evolution, role of acute rejection, risk factors, and impact on patient and graft outcome. *J Transplant*. 2015;2015:163757.
47. Ojo AO, Wolfe RA, Held PJ, et al. Delayed graft function: risk factors and implications for renal allograft survival. *Transplantation*. 1997;63:968–974.
48. Shoskes DA, Cecka JM. Deleterious effects of delayed graft function in cadaveric renal transplant recipients independent of acute rejection. *Transplantation*. 1998;66:1697–1701.
49. Troppmann C, Gillingham KJ, Benedetti E, et al. Delayed graft function, acute rejection, and outcome after cadaver renal transplantation. The multivariate analysis. *Transplantation*. 1995;59:962–968.
50. Yarlagadda SG, Coca SG, Formica RN Jr, et al. Association between delayed graft function and allograft and patient survival: a systematic review and meta-analysis. *Nephrol Dial Transplant*. 2009;24:1039–1047.
51. Chapal M, Le Borgne F, Legendre C, et al. A useful scoring system for the prediction and management of delayed graft function following kidney transplantation from cadaveric donors. *Kidney Int*. 2014;86:1130–1139.
52. Irish WD, Ilsley JN, Schnitzler MA, et al. A risk prediction model for delayed graft function in the current era of deceased donor renal transplantation. *Am J Transplant*. 2010;10:2279–2286.
53. Jeldres C, Cardinal H, Duclos A, et al. Prediction of delayed graft function after renal transplantation. *Can Urol Assoc J*. 2009;3:377–382.
54. Irish WD, McCollum DA, Tesi RJ, et al. Nomogram for predicting the likelihood of delayed graft function in adult cadaveric renal transplant recipients. *J Am Soc Nephrol*. 2003;14:2967–2974.
55. Kers J, Peters-Sengers H, Heemskerk MBA, et al. Prediction models for delayed graft function: external validation on the Dutch Prospective Renal Transplantation Registry. *Nephrol Dial Transplant*. 2018;33:1259–1268.
56. Zaza G, Ferraro PM, Tessari G, et al. Predictive model for delayed graft function based on easily available pre-renal transplant variables. *Intern Emerg Med*. 2015;10:135–141.
57. Rao PS, Schaubel DE, Guidinger MK, et al. A comprehensive risk quantification score for deceased donor kidneys: the kidney donor risk index. *Transplantation*. 2009;88:231–236.
58. Kamps JJAG, Hopkinson RJ, Schofield CJ, et al. How formaldehyde reacts with amino acids. *Commun Chem*. 2019;2:126.
59. Donate-Correa J, Matos-Perdomo E, Gonzalez-Luis A, et al. The value of Klotho in kidney transplantation. *Transplantation*. 2023;107:616–627.
60. Graver AS, Lee D, Power DA, et al. Understanding donor-derived cell-free DNA in kidney transplantation: an overview and case-based guide for clinicians. *Transplantation*. 2023;107:1675–1686.
61. Koyawala N, Reese PP, Hall IE, et al. Urine injury biomarkers are not associated with kidney transplant failure. *Transplantation*. 2020;104:1272–1279.
62. Zubair H, Azim S, Maluf DG, et al. Contribution of proteomics in transplantation: identification of injury and rejection markers. *Transplantation*. 2023;107:2143–2154.